MA50176 **Yang Zhou**
Instructor: Carlos Galeano Rios Due Date: 16/03/2018

Case Study 1: Industrial study on modelling heat sink

1 Problem Background

In physicists point of view, this world can be illustrated as a picture that contains huge numbers of systems and those systems interact with each other either by work or by thermal interactions to transmit energy. [1, p17] Therefore, heat transmitting is an important phenomenon that exist in our daily life and many industry productions process. In order to understand the modeling of heat transmitting we have chosen an important and commonly used electronic device - the heat sink - to understand how to build a simple mathematical physics model to describe the phenomena.

To build a mathematical model for a physical event, we naturally need to build the relationship of the maths concepts and equations with relevant fundamental physical laws. This relationship can be either local or global in space. Additionally it can be within a certain instant or a period of time. When we apply differentiation of physical variables with respect to time and space coordinates, the maths equations are describing the local region relationships among those physical variables in space and time, whereas the solutions represent the global relationships. Therefore we need to approach a maths-equation system under the restrictions of certain conditions (e.g. initial conditions or boundary conditions) to derive the global relations for a special physical event located at a corresponding local region at the instant time.[13, p11-12]

The above argument supports the possibility of linking the abstract maths concepts with real life situations. Therefore we can accept that an intuitive model is to use the heat equations, and we will in this case study steps of how the heat equations can be derived from a simplified physical model in 1-D world.Then we use the finite different method to approach the 1-D problem numerically as well as mathematical analytic reasoning.

The object of this case study is aiming to:

(I) formulate a simple mathematical physical model of heat transmission in heat sinks

(II) gain understanding in maths modeling methodology and some important approaches to model a real life phenomenon;

(III) compare the results of analytic approaches and numerical methods to a differential-equation system(the maths model);

(IV) gain some insight in how a extremely simple model can give useful insights to real life complex situations

At the end, the case study will use the modeling results to give some short discuss regarding possible further modeling directions.

1.1 Importance of Heat Sinks

The efficiency of removing heat generated by appliances (such as computers) dominates the reliability of these electric systems and of the possibility of minimizing the size of new generations of computers. [4]

Since the first digital computer in early 20s, the size of those original giants could be reduced in the first step due to the the invention of transistors which replaced the original vacuum-tube cooling system that took a huge space in those original electric computers. Following was new technologies in packaging more and more transistors on printed circuit boards and later on ceramic substrates.These packing engineering improved computer speed and storage capacity. Started from 1960s, the number of devices per chip increased from one to hundreds. New technologies in the 70s pushed the capacity to thousands of devices per chip. By 2010, the introduction of the microprocessor allows a chip contains about a billion transistors. The higher circuit packaging density has been accompanied by increased power dissipation per circuit in order to reduce circuit delay therefore to assist to increase circuits' speed. [4]

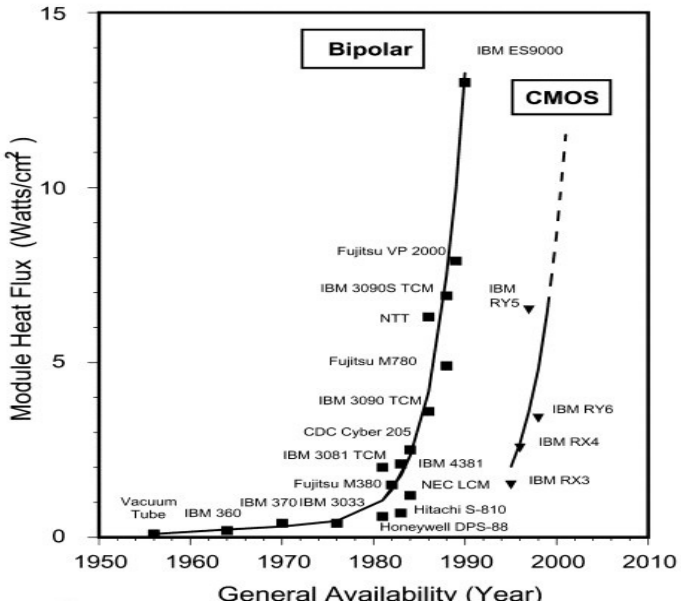

Figure 1.1: Evolution of module level heat flux in high-end computers.[4, page 1]

Figure (1.1)shows module heat flux associated with the advance of circuit packaging technologies. The heat produced by chips raised steadily before late 70s and turned to soar since 80s. Therefore the studies of heat sinks have been an extremely important discipline in electric engineering and electrical device production for decades.[4]

1.2 Illustrations

A heat sink (or heat spreader) is a kind of electronic device which can contain a fan or another type of cooling device to help transmit away the heat produced by a hot component (e.g a computer memory) more efficiently. Therefore it can be found in most appliances. Heat sinks can be either active or passive, defined respectively by whether

they use energy supply to power their mechanical parts in order to cool the hot component or not. The latter or passive heat sinks are mainly fin-shaped aluminum radiators that dissipates heat through the convection process. [3]

The below picture is a 2-D diagram of a passive radiator of finned aluminum. Our study will focuses on modeling the simple sinks first, then extend the active heat sink with an extra cooling system. Further we will also discuss the choice of materials for making heat sinks among aluminum, copper and iron.

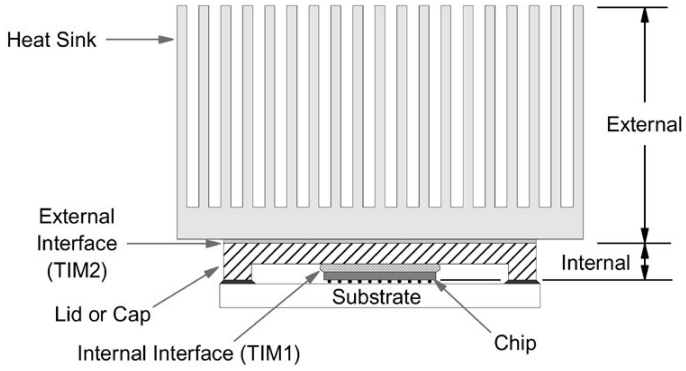

Figure 1.2: Cross-section of a typical module denoting internal cooling region and external cooling region.[3]

2 Problem formulation

2.1 Physical Model

One important method used for scientific studies is to simplify the phenomenon such that it can be translated to a systemically structured maths problem. Based on the simpler problem, an easy model can be built to test some most general and common characteristics of the object being studied. Following this philosophy, we consider the aluminum heat spreader is of the shape of a box of height L, as shown in the Figure (2.1) and the heat producer is closely connected to the spreader at its bottom. When we consider the small cylinder part in the middle of the spreader, we can ignore the influence of the side surface boundaries affect. If we can assume that the temperature at the bottom touching the chip is T_0 and the at the top surface touching the air is T_L, the overall heat flow should be dominated by the temperature difference between the bottom and the surface. Due to the fact that energy difference resulted from the higher temperature on bottom surface and the cooler room temperature at the top surface, there is a overall heat flux p, which is perpendicular to the paralleled top and bottom surfaces.

To see why we can simplify the heat flux direction only pointing from the box bottom to the box top, let us consider the situation that we take two close bars (A and B) from the middle location of the aluminum box in the above Figure (2.1). So in the Figure (2.2), heat exchange in other directions does exist, but aluminum is isotropic material (Refer to the definition 2.3.1 on page 6), and the temperature difference can be small between any two close bars, the non-vertical heat flux out from A to other bars can be cancelled out by other equally heat fluxes into bar.

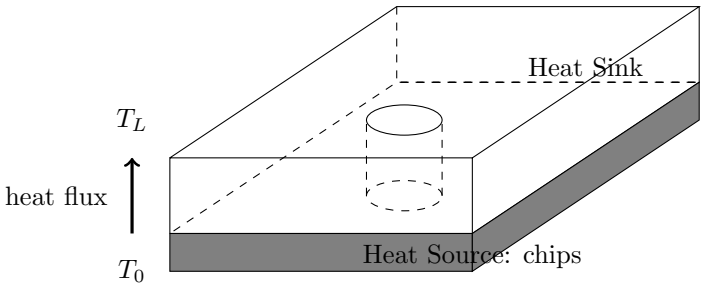

Figure 2.1: A simplified rectangular-shaped heat sink connected with a heat producing chip at the bottom

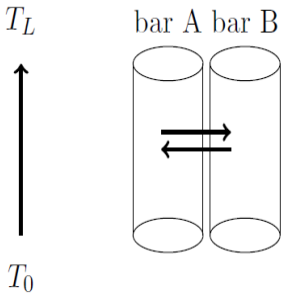

Figure 2.2: Inter-exchanging of heat among aluminum bars is in equilibrium, so we only consider the overall vertical heat flux from bottom to top, i.e. from higher temperature to low temperature.

2.2 1-D Model

The first step is to develop a one-dimensional (1-D) model of the heat flux changes. Taking a bar of the metal from the middle location of the box, like the little cylinder in Figure (2.1), we have the new 1-D graph in Figure (2.3):

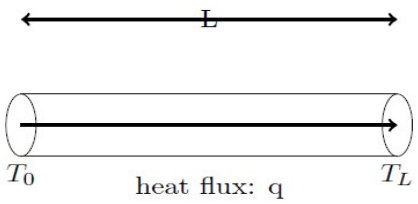

Figure 2.3: A 1-D model of heat sink

The T_0 is the temperature connected to the heat source and T_L is the top edge at the heat sink. This 1-D heat sink only absorbs heat from a heat source located at point of T_0 and contains no internal heat source (with reference to equation (2.2)) can be described by the model(1a), (1b), (1c) and (1d):

$$\partial_t T = K \partial_{zz} T, \text{ with } z \in [0, 1] \tag{1a}$$

where $K = \frac{k}{\rho C}$

$$T(z, 0) = T_\infty, \tag{1b}$$

$$T(0, t) = T_\infty + D(1 - e^{-t/\tau}), \tag{1c}$$

where T_∞ is the room temperature.

$$\frac{hT}{k} + \partial_z T(L,t) = \frac{h}{k} T_\infty \tag{1d}$$

Details of the meaning of the above equations (1a) to (1d) will be explained in the next section. All the proofs will be involved in appendix sections. Notations and meanings can be found in the Nomenclature table on page 33.

2.3 Governing principles

Building mathematical models using physical laws means establishing relations or equations that have physical meanings at a point in space and at an instant in time.[13, p12] Therefore the instant states of physical points in a system is the starting point to formulate maths equations.

We can apply physical laws to a physical point in space and an instant in time to derive the equations. Since those laws are generally applied in a material system and a process, therefore the physical point is defined to be located within a extremely small and special region. Likewise we define the time instance as a extremely short and temporal time period.[13] For example, in our 1D model: a point on the bar with coordinate z means the region$(z, z+\Delta z)$, where $\Delta z \to 0$; the time instance t represents the short time period from t to $t + \Delta t$, with $\Delta t \to 0$. [13]

Under such reasoning, our modeling process needs the clarification of several important physical laws: the conservation of energy, Fourier's law of conduction, Newton's cooling law and three heat-transferring mechanisms. Those concepts are explained in the following subsections.

2.3.1 The first Law of Thermodynamics

Commonly known as the law of *conservation of energy*, this law states that a given system always has the same total energy or *internal energy* associated with it when it does not interact with another system. The symbol of internal energy is U with a common unit the joule. [1] And this law gives the follow *energy equation* for the inner energy of a body:

$$\rho c \cdot \partial_t T + \nabla \cdot q = F(M,t), \tag{2.1}$$

where ρ and c are the density and the specific heat of the material, F the rate of internal energy generation per unit volume. [13]

By using the Fourier's Law equation (2.4), we have the *classical parabolic heat-conduction equation* :

$$\partial_t T = K \triangle \cdot T + \alpha F, \tag{2.2}$$

where $K = \frac{k}{\rho c}$, $\alpha = \frac{1}{\rho c}$,and $\triangle \cdot T$ is applying the gradient operator ∇ twice on T. In Cartesian system:

$$\triangle T = \nabla(\nabla \cdot T) = \nabla \begin{bmatrix} T_x \\ T_y \\ T_z \end{bmatrix} = \begin{bmatrix} T_{xx} \\ T_{yy} \\ T_{zz} \end{bmatrix}. \tag{2.3}$$

2.3.2 Fourier's Law of Conduction

Definition 2.3.1 *A material is said to be isotropic when it behaves all the same in all different directions[1]. A homogeneous and isotropic solid is defined as a type of material that its thermal conductivity is independent of direction within the solid.*

For such a solid, the heat flow and the temperature gradient have the follow relation[13]:

$$q(M,t) = -k\nabla T(M,t), \tag{2.4}$$

where the *temperature gradient* ∇T is a vector normal to the iso-thermal surface; the *heat flux* $\mathbf{q}(M,t)$ is the flow of heat per unit time, per unit area of the iso-thermal surface of the direction of the decreasing temperature; k is the *thermal conductivity* of the material.[13] The thermal conductivity depend on the in location in space, but for isotropic system it is a positive scalar. The above relationship is the Fourier's law of conduction or the *constitutive relation of heat flux*. In a Cartesian system, this constitutive relation can be re-written as:

$$\mathbf{q}(x,y,z,t) = -k(\partial_x T \cdot \mathbf{i} + \partial_y T \cdot \mathbf{j} + \partial_z T \cdot \mathbf{k}), \tag{2.5}$$

where $\mathbf{i}$, $\mathbf{j}$ and $\mathbf{k}$ are the unit direction vectors along the x, y and z directions respectively.[13]

In our special 1-D model, we keep only one direction $\mathbf{k}$, so the above equation (2.3.2) is in the form:

$$\mathbf{q}(z,t) = -k(\partial_z T\mathbf{k}), \tag{2.6}$$

The proof can be found in the Appendix on page 25.

2.3.3 General Nature of Thermal Radiation

Heat is transferred in three types of mechanics: *conduction*, *convection*, and *radiation*. The first two ways need the present of matter, whereas the latter needs no media.

> In conduction, thermal motions diffuse through the substance, and convection involves bodily movement in a fluid.[1, p90]

To be more explicit, in conduction process, the temperature difference inside a material or *temperature gradient* forms a driving force to have heat flow from higher gradient to the lower. For heat flow, the rat of heat flow per unit area Q is proportional to the magnitude of temperature gradient. This is the relation called Fourier's law of conduction.[1]

Convective heat transfer or *convection* is the heat transmitting process involving interacting with flow of fluids. In the simple case, we assume that the fluid or air in the heat sink example, is forced to move with external mechanisms. Therefore, there is friction when the two system meet at the solid's surface. Based on classical mechanics, on the surface of the body, we can assume that the fluid stuck to the solid surface with no-slip friction. This is the *no-slip hypothesis*. Therefore within a extremely small distance ϵ above the sold wall, the fluid has no velocity and no motion. For this layer, the heat conduction will apply:[2]

$$q = -k(\frac{\partial T}{\partial \epsilon})|_{\epsilon \to 0^+}. \tag{2.7}$$

For the layer of fluid that is not motionless, the pure heat conduction can no longer be applied. In order to proceed we need the experimental classical law of convection, also called *the Newton's law of cooling.*

Newton's Cooling Law states that:

> the change in an object's temperature is proportional to the difference between its own and the ambient temperature.

[5] This law is obtained through experiment observations. In equation is:

$$Q \propto T_s - T_\infty, \text{ where } T_s \text{ is the surface temperature.} \tag{2.8}$$

$$Q = h(T_s - T_\infty), \text{where } h \text{ is the heat transfer coefficient} \tag{2.9}$$

By considering momentum equation caused by the skin friction when fluid passes the surface of a body, the heat transfer coefficient is derived to be:[2]

$$h = \frac{-k(\frac{\partial T}{\partial \epsilon})|_{\epsilon \to 0^+}.}{T_s - T_\infty} \tag{2.10}$$

This law is describing convection process also called *Robin's boundary conditions.* More details about the proof of convection can be found in the book by Bejan (2013) [2, p32-34].

2.4 Conditions for Determining the Solutions

Mathematical physical models describes the the global truth of physical laws, but the physical problem which is formed by a special phenomenon is located within a special region of space and time.[13] Therefore, even though the groups of solutions from the model are derived, we still need to special registrations to filter the relevant solutions for the spacial given event. Additionally, heat conduction equations without their solutions can only describe how temperature behaves within a system, but cannot show how the temperature is distributed. In order to obtain the distribution, certain initial and boundary conditions need to be stated clearly before solving the equation systems.[7, p10]

2.4.1 Initial Conditions

Initial conditions or *Cauchy conditions* are temperature values of a system at the beginning of time when the system is observed, t_0= 0 s.[11] When heat is conducted in a solid bar, the bar's temperature tend to a constant T_0, which is the mean value of temperature over the rod. Or the initial temperature distribution can be written as:

$$T(M, 0) = \varphi(M).$$

This is the initial state of the whole system. Physically the meaning of initial conditions depends on physics and nature of the variable T. In this solid bar case, the distribution should be constant temperature without any external decaying forces. Especially consider that we take a sufficiently long time to be the initial point, the system itself should be in a thermal static state, which is a constant. [13]

Since we have mentioned that physical phenomenon is relatively local in space and time, later in our model validation, we will see a simple example with a special heat distribution within the body. This is done for the testing purpose. That initial temperature is different from our definition here because that can be considered as a metal bar being heated in some point or points then being taken away from the heat source. This is with a shift in time, so the event has changed.

2.4.2 Boundary Conditions

Our model is 1D, so the length parameter z is in the domain $[0, L]$. In our 1-D model diagram (Figure 2.3), we call the temperature at $z = 0$ be $T(0, t) = T_0$ and at $z = L$ be $T(L, t) = T_L$ only for simplicity of notation. It does not mean the two boundaries have constant temperature values. However those should be perceived as at that special time instant, some possible temperature values at the ends are assumed to be T_0 and L_L.

To be more precise, boundary of a system is the end point(s), boundary curve(s) or boundary surface(s) of the body. Since our model is in one dimensional space, the boundary considered in our report is referring to the end points. Boundary conditions therefore specifies situations of, or constrains on those dependent variables in our model on the system boundary. [13] There are typically four types of boundary conditions: Dirichlet conditions, Neumann conditions, Robin condition and boundary conditions for meeting surfaces problem of two or more systems'. [11], In our report we include only the first three conditions due to the simplicity of those conditions.

Dirichlet boundary In a general three-dimensional system, the inner domain is denoted as Ω and the boundary surface is denoted as $\partial\Omega$. Assuming that the surface temperature can be expressed by some known function $\varphi(S, t)$, S *in* $\partial\Omega$ [13], this known boundary temperature distribution is the *Dirichlet boundary condition.* It is expressed by:

$$T(S, t)|_{\partial\Omega} = \varphi_{\partial\Omega}(S, t)$$

[11] In one-dimensional case, the equations for the temperature on two end points are:

$$T(z, t)|_L = T(L, t)$$
$$T(z, t)|_0 = T(0, t),$$

where both $T(L, t)$ and $T(0, t)$ are known from measurement. Additionally, we assume that Dirichlet conditions mean that there is a upper or lower limit of the know temperature function.We can use this Dirichlet boundary condition to model temperature at the bottom of the heat sinks, since chips have sensors to measure and give instant temperature values. In our model, we express it in the model as equation (1c).

Neumann boundary conditions In many situations, it is not always possible to have mensurable temperature values on the boundaries. In some applications, boundary conditions are instead given by directional derivative along outward normal vectors on the the boundary.[13] In practice is when the heat flux from a body surface can be obtained from measurements[11]:

$$k \nabla T \cdot \mathbf{n}|_A = q(\mathbf{r}_A, t).$$

In Cartesian system, such situation can be expressed as:

$$\left(k_{xx}\frac{\partial T}{\partial x}n_x + k_{yy}\frac{\partial T}{\partial x}n_y + k_{zz}\frac{\partial T}{\partial x}n_z\right) = q(\mathbf{r}_A, t), \tag{2.11}$$

where $\mathbf{r}_A$ is a positional vector of a point located at the boundary surface. This boundary condition is commonly applied on the surface of radiate systems. [11] For isotropic system, the above equation (2.11) becomes:

$$\left(k\frac{\partial T}{\partial n}\right)|_A = q(\mathbf{r}_A, t). \tag{2.12}$$

This equation (2.12) can be applied to a static system and transient inverse heat conduction problems.[11]

When insulator covers certain surface area of a system, we consider that there is no neat transmission on those surface areas to the insulator, or no heat flux flowing though the ares:

$$\frac{\partial T}{\partial n}|_A = 0.$$

[11]

In one-dimensional space, a directional derivative is expressed by a partial derivative with respect to the length z, because we need to consider the influence of time. This can be expressed similarly as in a isotropic system (Refer to definition 2.3.1 on page 6) in equation (2.12). [13]

The Dirichlet and Neumann boundaries are easy to solve but have certain restrictions when applying. In order to use these two conditions, we need to assume that the thermophysical properties of the body c, ρ and k are temperature *invariant* (not changing with the change of temperature).[11]

Robin boundary conditions The *Robin boundary* is also know as the *Newton law of cooling*.[11]

This boundary is to model the heat transmission on a surface interacting with another fluid. From Newton's law of cooling, we have the equations (2.8). From Fourier's law, we have the heat flux equation determined by gradient of Temperature. As explained in the convection law subsection, we can assume that the thin layer of fluid on solid wall have both the conduction and conviction law due to the non-slip friction hypothesis. Therefore:

$$-k\nabla T\mathbf{n} = h(T_{s,t} - T_\infty)\mathbf{n} \tag{2.13}$$

$$-k\partial_z T = h(T_{s,t} - T_\infty), \text{ in 1-D model.} \tag{2.14}$$

By dividing both sides of (2.14) by the constant k and take the length location of the end point to be L as in our model, we will obtain the last equation (1d) in our original model. We use this Robin boundary to model the upper surface's heat convection with the flowing air.

2.5 Non-dimensionalisation

Since we are building mathematical physical models, all the variables are of physical meanings. This means all quantities have their special units. Especially when we apply

differentiation of physical variables with respect to time and space coordinates, the maths equations are describing the local region relationships among those physical variables in space and time. However the followed solutions represent the global relationships among variables in space and time.[13] Therefore, due to the need of expressing true facts, we need to take away the units for each physical variables to maintain the philosophy that those equations are true under different measurement or units. And we use solidus notation to keep those variables dimensionless.(Definition and meaning of solidus notation see page 27) Thus it is a common practice to non-dimensionlisation the equations by changing of variables to take away the units and turn the quantity-value to be pure numbers.

In our original model (1a) to (1d), Since without any external heat, the temperature of our heat sink will always be the same as the room temperature. Define $T^{'} = T - T_{\infty}$ gives $T = T^{'} + T_{\infty}$, and substitute back to (1a) to (1d) gives:

$$\partial_t T^{'} = \frac{k}{\rho c}\partial_{zz} T, \tag{2.15}$$

$$T^{'}(z,0) = 0, \tag{2.16}$$

$$T^{'}(0,t) = D(1 - e^{-t/\tau}), \tag{2.17}$$

$$\frac{h}{k}T^{'}(L,t) = -\partial_z T^{'}(L,t), \tag{2.18}$$

From the above model, we can see that the units of variables T', z, and t are:

$$[T'] = D, \quad [z] = L, [t] = \tau \tag{2.19}$$

To derive the dimensionless model, we should remove the influence of those units by defining the following dimensionless parameters:

$$\begin{cases} T^* = \frac{T^{'}}{D}, \ , \quad z^* = \frac{z}{L} \\ t^* = \frac{t}{\tau}, \\ F_0 = \frac{k\tau}{\rho c L^2}, \quad B_i = \frac{hL}{k} \end{cases}$$

Through some algebraic calculations, and removing the $*$ from the variables, the final dimensionless maths model is obtained as listed below:

$$\partial_t T = F_0 \partial_{zz} T, \tag{2a}$$

$$T(z,0) = 0, \tag{2b}$$

$$T(0,t) = 1 - e^{-t}, \tag{2c}$$

$$B_i T(1,t) = -\partial_z T(1,t). \tag{2d}$$

The calculation process to derive this dimensionless model from the original model can be found in Appendix B on page 27.

3 Solution of the Model Problem

In practice, most of the differential equations for physical models may not have exact analytically solutions. Or the solutions could be difficult to comprehend. Under such

situations, numerical approaches offer a easier and clearer way to obtain further interpretation from the model. [12] To approach a problem numerically, we first need to reduce the infinitely continuous domain space to a discrete space. There are several finite methods and accordingly different ways can be applied to reduce the infinite domain to a finite one. In this case study, we will use the Crank Nicolson finite difference method. This method is valid and do not require a really small grid length. More details about Crank-Nicolson implicit method can be found in the book by Smith[10]: the scheme driving process on page 19 to 24; derivative boundaries on page 29 and page 30; The convergence and stability of solutions simulated by finite difference methods on page 43 to 49.

3.1 Numerical Approach-the Crank-Nicolson Finite Difference Method

To approach the problem using numerical methods, we need to put the non-dimentionalized models into the *finite difference* scheme. Therefore computers can simulate the infinite event in a discrete system. To do this we need to place the domain in a discrete grid. For simplicity, we choose the uniform grid in space and time. In our one-dimension model, we take finitely many equally distanced points on the bar (e.g take distance spacing $\Delta z = 0.1cm$)and measure the temperature on each points and their temperature changes with certain time intervals say take the time spacing $\Delta t = 0.1s$. [12] To illustrate this method, see Figure 3.1b bellow:

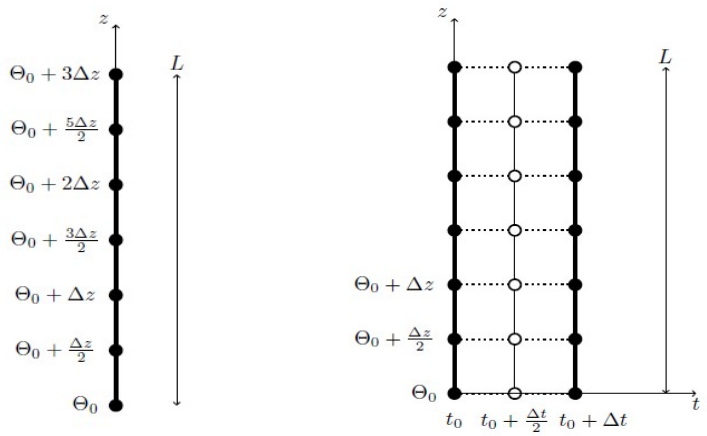

(a) Discrete grid graphs of temperature $\Theta(z)$ with grid length $\Delta z/2$

(b) Finite different method: grid graphs of temperature $\Theta(z)$ with discrete change of time Δt

Figure 3.1: Finite different methods

The Figure 3.1b shows the one-dimension bar with length L set to grids with equal length of $\Delta z/2$. And Figure 3.1b expands the grid to the space-time domain, with equal time increment $\Delta t/2$. We label the nodes on the lattices from bottom to top (n_i, $i = 1, ..., 7$) and from left to right (n_{i+7}, n_{i+14}) as in Figure 3.2.

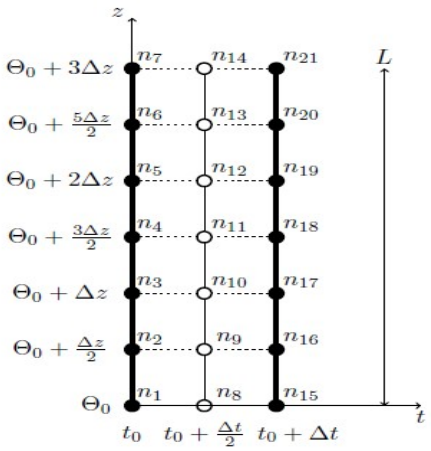

Figure 3.2: Finite different method: grid graphs of temperature $\Theta(z)$ with discrete change of time Δt with labeled nodes

The domain can be approached by approximating the solution of our model at the nodes on the lattice. Therefore, define the function on black node n_i to be $\Theta(z,t)$. For example, we have temperature measured at nodes n_1, n_3, n_{15} and n_{17}. With those values we can approximate the modeled temperature at node n_9:

$$\partial_t \Theta(z,t) = \frac{\Theta(z,t+\Delta t/2) - \Theta(z,t-\Delta t/2)}{\Delta t} + o(\Delta^4), \tag{3.1}$$

$$\partial_{zz} \Theta(z,t) = \frac{\Theta(z+\Delta z/2,t) - \Theta(z-\Delta t/2,t)}{\Delta z^2/2} \tag{3.2}$$

$$\partial_{zz} \Theta(z,t) = \frac{\partial_{zz}\Theta(z,t+\Delta t/2) - \partial_{zz}\Theta(z,t-\Delta t/2)}{2} \tag{3.3}$$

After calculation we have the following expression for all interior nodes:

$$\varphi_i^{k+1} - \varphi_i^k = \frac{F_0 \Delta t}{2\Delta^2}\left[\varphi_{i+1}^{k+1} - 2\varphi_i^{k+1} + \varphi_{i+2}^k - 2\varphi_i^k + \varphi_{i-2}^k\right] \tag{3.4}$$

Similarly, adding boundaries to boundary nodes according to the need of model(Dirichelt, Neumann, or Robin conditions). And turn the expanded system to MatLab codes for simulations.
Calculation details can be found on book by Thomas[12, p6-14]. All used Matlab codes can be found in Appendix C on page 29.

3.2 Validating the Numerical Method

In order to check the validity of our numerical methods, we first derive the exact solutions of a simplified Neumann-Neumann boundary problem and then compare the analytical results with the accordingly altered numerical method.

3.2.1 Analytically Approach of a simple example

Figure 3.3 is the simplified model. We set the two boundary temperature distribution functions to be zero. The initial state for the inner system is given with a special heat

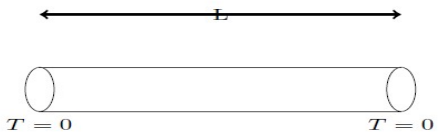

Figure 3.3: A bar with initial non-even Temperature distribution over the body, but the ends have temperature fixed as 0

distribution $f(z)$. According to the initial and boundary conditions of this simple system, we have our original model (2a) to (2d) altered to be the following:

$$T_t = F_0 T_{zz},\ z \in (0,1) \tag{3.5}$$
$$T(z,0) = f(z),\ z \in [0,1] \tag{3.6}$$
$$T_z(0,t) = 0,\ t \in [0,1] \tag{3.7}$$
$$T_z(1,t) = 0,\ t \in [0,1] \tag{3.8}$$

For such system of partial differential equations, We can approach it by the method of separation of variables. Therefore, the ansatz of the solution takes the form:

$$\Theta(z,t) = S(z)\mathcal{T}(t)$$

Take derivatives with respect to t and zz gives:

$$\Theta_t = S(z)\mathcal{T}_t(t) \tag{3.9}$$
$$\Theta_{zz}(z,t) = S_{zz}(z)\mathcal{T}(t) \tag{3.10}$$

Substitute (3.9) and (3.10) to the above model, gives:

$$S(z)\mathcal{T}_t(t) = F_0 S_{zz}(z)\mathcal{T}$$
$$S(z)\mathcal{T}(0) = 0$$
$$S_z(0)\mathcal{T}(t) = 0$$
$$S_z(1)\mathcal{T}(t) = 0$$

With some algebraic calculation gives:

$$\frac{\mathcal{T}_t(t)}{F_0\mathcal{T}(t)} = \frac{S_{zz}(z)}{S(z)} = c, \text{c is a constant} \tag{3.11}$$
$$\mathcal{T}(0) = 0 \tag{3.12}$$
$$S_z(0) = 0 \tag{3.13}$$
$$S_z(1) = 0 \tag{3.14}$$

Seperate the equation (3.11) to two different equations and integrate over both of them. Applying the three conditions (3.12), (3.13) and (3.14) to the solutions and checking the

validity. Eventually we drive the exact solution:

$$S_n(z) = C_n cos(n\pi z) \tag{3.15}$$

$$\mathcal{T}_n(t) = D_n e^{-\pi^2 n^2 F_0 t} \tag{3.16}$$

$$f(z) = \sum_{i=i_0}^{i_{final}} E_n cos(n\pi z) \tag{3.17}$$

$$\Theta(z,t) = \sum_{n=i_0}^{i_{final}} E_n cos(n\pi z) e^{-\pi^2 n^2 F_0 t}. \tag{3.18}$$

Existence and Uniqueness of the solution The series is unique and (3.18) converges to the real solution of the simple problem. The existence and uniqueness of the exact solution has been a well studied problem, so details of proof will not be involved in this report. Relevant proofs can be found in the book by Wang[13, p122-125].

3.2.2 Numerical simulation of the simple system

This section is to check the validity of our model developed at the beginning of the section. To check the validity, we compare the analytical solution of the simple event to the numerical solution of (3.18) for a bar of aluminum using MatLab. The end points temperature values are both set to be 0.

Before running simulation, we need to specify a few constants which will be used in our model. The materials we have chosen are aluminum and copper over iron, because the former two have higher k value under the same temperature conditions, as shown in Table 1:

Table 1: Thermal Conductivity constants k for aluminum, copper and iron under different temperature values[16]

Metal	Temperature K	Equivalent T in (°)	Thermal Conductivity k (W/mK)
pure Aluminum	68	20 to 25	204
	200	93	215
pure Copper	68	20	386
pure Iron	68	20	73

In Table 2 are the density constants ρ and in Table 3 are the values of specific heat for different metals:

Table 2: density constants ρ for aluminum, copper and iron[17]

Metal	Density (kg/m^3)	Metal	Density (kg/m^3)	Metal	Density (kg/m^3)
Aluminum	2712	Copper	8940	Iron	7850

Table 3: Specific Heat constant c for aluminum, copper and iron[18]

Metal	Specific Heat c_p (kJ/kgK)
Aluminum	0.91
Copper	0.39
Iron	0.45

3.3 Validity of the Numerical Approach

In order to check our numerical method, we need to compare the numerical solution to our exact solutions of the simple Neumann-Neumann example in page 12. We keep the material to be aluminum. For the choice of constants, we have after the change of units: the thermal conductivity $\frac{k}{KJ/(s \cdot m \cdot K)}$: 0.204; the density $\frac{\rho}{kg/m^3} = 2712$; the specific heat $\frac{c_p}{KJ/(kg \cdot K)} = 0.91$; We set the time scale $\tau/(s) = 1$ and metal length $L/(m) = 0.01$. The Fourier Number F_0 is therefore 0.8266. We also need to check the unit dimensions in calculation gives a unitless constant F_0:

$$[F_0] = \left[\frac{k\tau}{\rho c_p L^2}\right] = \frac{[k\tau]}{[\rho c_p L^2]} = \frac{KJ/(s \cdot m \cdot K) \cdot s}{(kg/m^3)(KJ/(kg \cdot K))(m^2)} = 1$$

We need to alter the numerical MatLab Code to 0 valued Neumann conditions. Then the numerical simulation give the following graphs:

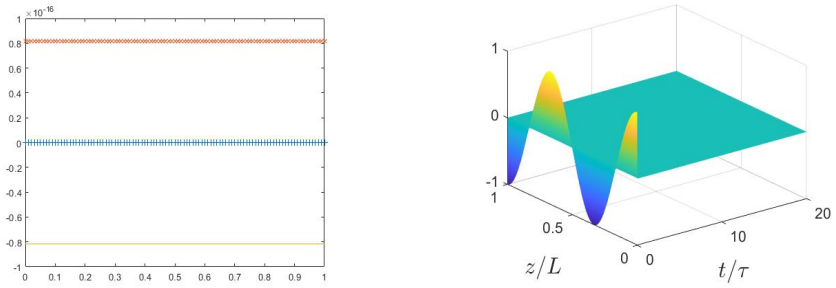

(a) Simulation errors VS the exact solution **(b)** Temperature changes on the metal bar over time

Figure 3.4: comparison of the exact solution and the numerical simulation

The mean squared error is 6.6594e-33. Therefore we have checked that this numerical method gives accurate approximation of our simple example. (This MatLab code is in Appendix C: Validity Checking on page 29)

4 Results and Interpretation

4.1 Simulation of Dirichlet-Dirichlet conditioned models

We have checked the validity of our numerical methods, therefore we can proceed to run another simpler simulation of our model under Dirichlet-Dirichlet conditions on both ends. The result produced the two graphs in Figure 4.1.

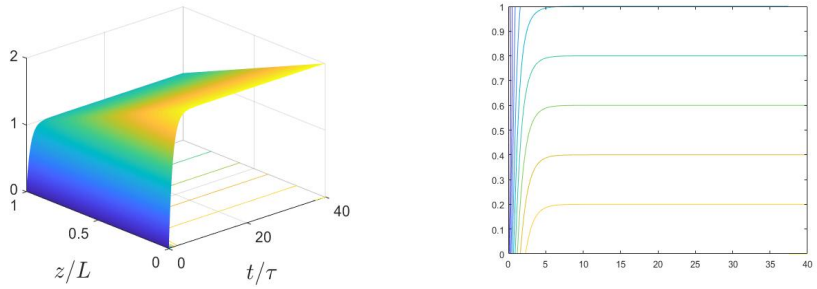

(a) Dirichlet-Dirichlet boundary heat conduction

(b) Dirichlet-Dirichlet boundary: Temperature contour plot

Figure 4.1: Simulation graphs for Dirichlet-Dirichlet problems

Figure 4.1a simulated the heat transmitting process along the aluminum bar with the change of time, conditioning on both ends under Dirichlet conditions. The temperature at $z = 0$ starts to increase as it starts to receive heat from the source. We can observe that temperature within the bar has a rapid increase then maintained at a relative steady state. Temperature at the end point $z = L$ also increases steadily as the time increases. This is a reasonable result since our system is isotropic.We can expect a steady heat flux between the two end points. This assumption can be proved by the contour plot in graph 4.1b.

One non-realistic part with this simulation is that: even though we can measure the temperature at the lower boundary and it is possible to keep it within a maximum temperature, it is not realistic to keep a constant temperature value at the upper boundary.Therefore this is not a better model compared to our original proposal of applying Dirichlet-Robin conditions. However before simulating the original model, we test with non-zero Neumann-Neumann conditions.

4.2 Simulation of the Neumann-Neumann conditioned models

The second simulation is model heat sinks under non-zero Neumann-Neumann conditions at both ends. This is an updated model from the original simple validation simulation. The Temperature distribution along the bar with respect to the change of time is plotted below:

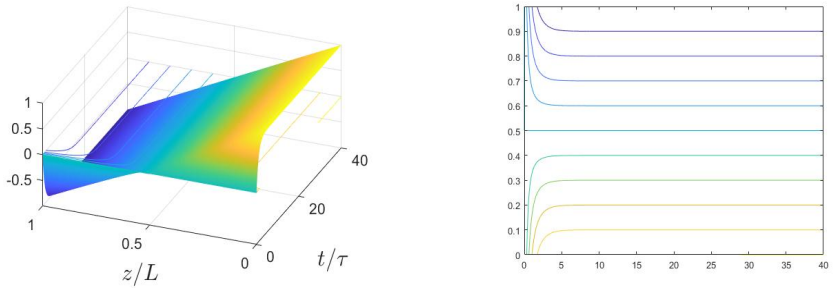

(a) Neumann-Neumann boundary heat conduction

(b) Neumann-Neumann boundary : Temperature contour plot

Figure 4.2: Simulation graphs for Neumann-Neumann problems

Since both ends are fixed with a constant heat conduction speed, we expect to see that after temperature rising within the beginning time instant, the system's temperature should be linearly distributed. This assumption is proved by the two graphs in Figure 4.2. The contour plots in graph 4.2b shows that after a time length around 5 seconds, the fast increasing temperature starts to main in a steady state.

However there is one observation does not match with our assumption for the heat sink model. We noticed that in graph 4.2a, the upper boundary temperature raised rapidly at during the first 5 seconds then turned and started to drop and reached minus temperature value. This could not be happening in our simple heat sink model. The cause of this wrong process is that in the Neumann boundary simulation, we keep both the heat flux entering and leaving the system as a constant. At the upper boundary, the system will therefore keep decreasing the temperature even when the upper boundary already reaches the room temperature. This is apparently not realistic.

One way to modify this is to consider turn off the upper cooling system when the temperature reaches 0(the relative room temperature after non-dimensionalisation process). However, since the heat is steadily flowing into the system at the lower boundary, the Neumann cooling process need to be turned on with a short amount of time. This is approachable but making our model much more complicated than intended. This is the reason we will run a third simulation using Dirichlet and Robin boundary conditions as we proposed in the original model.

4.3 Simulation of the Dirichlet-Robin conditioned model

In the second step, we simulate our original model using Robin condition on the top of the bar to approach a real life situation.

In this model, we consider the fluid flow at the end is due to extra mechanics. Therefore we need to consider the air heat transfer coefficients h in forced convection. We can check two different air flow movement and two liquids movement:

Table 4: heat transfer coefficient h for air and liquid under forced movement[15]

Fluid	movement speed	$h\ (W/sm^2K)$
Air	slow	10
Air	fast	100
Water in a pipe	fast	3000
Liquid	fast	10000

To calculate the Biot number, take aluminum thermal conductivity $k/(W/(s \cdot m \cdot K))$: 204 and bar length $L/(m) = 0.01$:

Table 5: $B_i number under different fluid movement$

Fluid	movement speed	B_i
Air	slow	4.902e-04
Air	fast	0.004902
Water in a pipe	fast	0.1471
Other liquid	fast	0.4902

From Table 4 and Table 5, we can see that the heat transfer coefficients h of slow air flow, fast air flow, fast water flow and fast other liquid flow are increasing. Accordingly, the Biot number B_i shows that the outer resistance of heat transmitting are higher in the air flow environment than the liquid flow environment. Therefore, we can reasonably deduce that air cooling effect should be less efficient than liquid cooling.

Alter the code to Dirichlet-Robin conditions and run the simulation under the four different Robin boundaries according to the different transfer coefficients h of four fluid movements. The changes of temperature value at the upper bound of our model against time is plotted below in Figure 4.3:

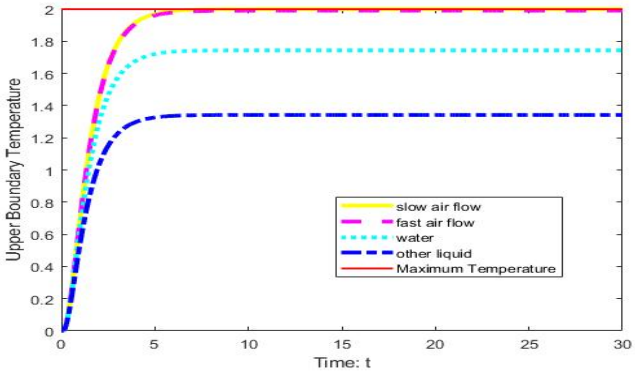

Figure 4.3: Changes of upper boundary temperature T_L alogn time t when cooled by four different fluid movements: slow air flow, fast air flow, fast water flow in pipes, and fast (other) liquid flow in pipes.

The Maximum temperature is the maximum value obtained at the lower boundary where heat is being absorbed. The four curves represent the temperature change at the upper bound when placed in four different fluid movements. The four have a similar behaving pattern: the temperature increases rapidly at the beginning as heat being absorbed but the temperature difference from the body to the cooling fluid are not big enough for convection to work efficiently. After some time length, when certain temperature is reached, stronger convection process starts to reduce the speed of temperature rising. This results matches our hypothesis based on the data from Table 4 and Table 4. This can be another way to support the validity of our numerical model.

However, there is one doubt raised from the above simulation result. The air cooling results are not good enough to prevent the equipment being burned hence this result cannot match with the common application of the combined cooling device of heat sinks and fans. Such cooling devices,which function based on natural and forced air flow, are commonly seen in personal computers. One explanation is that our simulation is only in one-dimension, and the heat convection process only works at the top point. Therefore heat cannot be transmitted away in other directions. One way to verify our guess is to plot the top temperature changes with respect to different bar length as in figure 4.4:

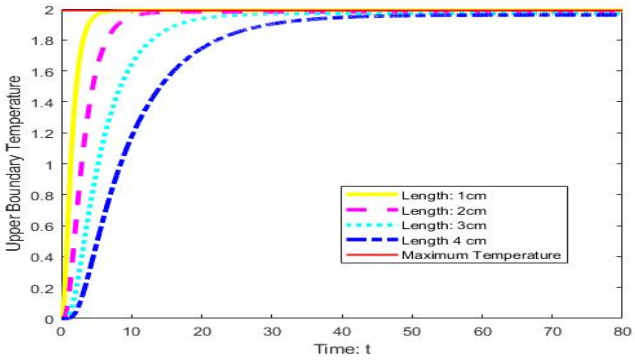

Figure 4.4: Comparing the changes of upper boundary temperature T_L along time t when in four models with different bar length: 1cm, 2cm, 3cm and 4cm. The four simulations were all in the environment of fast air flow.

We keep the four bars of length 1 cm, 2 cm, 3 cm and 4 cm all in the same fluid environment. As expected, the eventual temperature of should reach the maximum value regardless of the length of bar, because the heat convection process at the upper endpoint should be similar under small change of length. To see this, calculate ratio of the B_i number vs the bar length: $h/k = 0.4902$ (This is for placing a one-dimension aluminum bar in a fast air flow.) Since our change of length is around 0.01 m the total influence caused by increasing length over the ratio is rather small.

However, this result proposes an interesting assumption: in higher-dimension model, the simulation should show that fast air flow can efficiently transport the heat away from heat sink. Consider a two-D model of the shape as a rectangle. The fluid convection is now flowing around a rectangle or a squashed "cylinder". The transfer coefficient h for such situation increases to $200(W/sm^2K)$[15]. And since the fluid is working on three edges of the rectangle, with a good choice of volume-surface ratio, the system could be maintained within a safe temperature level for the electronic devices.

5 Further Modelling

In this section, we try to apply our model by altering some simple constants in the expression to model some different situations and hopefully can obtain some useful conclusions. We will first test the performance of heat sinks that made of three different metal materials. Second part, we will discuss briefly some further study possibilities based on all the simulation results.

5.1 Models of Different Materials

At the beginning we have chosen aluminum to be the material for the heat sink. A natural question to ask is whether other metal can be used to replace aluminum and have a better result. We choose to check three types of common metal: copper, gold and iron. And see which one can be a better material for heat sink.

Different metals gives different constants coefficients. In order to proceed the simulation. Taking the data from Table 1, Table 2, and Table 3, we can calculate the Fourier number F_0:

Table 6: Fourier Number F_0 for aluminum, copper and iron

Metal	F_0	Metal	F_0	Metal	F_0
pure Aluminum	0.8266	pure Copper	1.1071	pure Iron	0.2067

From the discussion section, we have seen that air has low efficiency for cooling our model. To make the comparison among different metals clear, we choose to use water as the cooling fluid. Therefore we can calculate the Biot number B_i:

Table 7: Fourier Number F_0 for aluminum, copper and iron

Metal	B_i	Metal	B_i	Metal	B_i
pure Aluminum	0.1471	pure Copper	0.0777	pure Iron	0.4110

5.2 Simulation Results

We run the simulations for the three metals and compare the boundary temperatures changes, boundary heat flux changes and average heat flux in the following four grouphs in Figure 5.1.

In Figure 5.1a plotted the temperature changes at the bottom point of all the three heat sinks. The curves all have the same behaviour with respect to time t. There is a rapid nearly linearly increase during the first 4 seconds. Then the temperature raise slows down and stays at the maximum temperature.

Figure 5.1b shows how the upper boundary temperature change along with time. The three curves represents temperature values at the upper point from the aluminum device, the copper device and the iron device. The three cures have similar trend: first increasing rapidly, and stay at a maximum steady temperature. However, we can see that the maximum temperature for each device are different. Aluminum reaches the highest value around 1.9(This is the dimensionless temperature value). Copper reaches the second highest around 1.75 and iron reaches 1.4 the lowest. This observation lead to a question: which metal is more efficient in conducting heat and able to keep our heat source device safe?

Those three sinks are placed inside the same heating and cooling environment. And from the heat absorbing point we can see from figure 5.1a there are no differences in efficiency among the sinks to absorb energy. Therefore, we can observe from the top boundary temperature. Based on Newton's cooling law, when the temperature difference is larger, the heat convection effect should also be stronger. Therefore we can roughly guess that the device with higher boundary temperature might indicate higher efficiency.

To test the plausibility of our explanation, we should test the strength of heat flux from our simulations, because base on Fourier's Law of conduction, stronger heat flux means more energy being transported away within a unit area and unit time period. Therefore the upper boundary heat flux and the average heat flux over the entire bar are plotted in graph 5.1c and graph 5.1d respectively.

In graph 5.1c, the upper heat flux cures were plotted for all those three metal sinks.

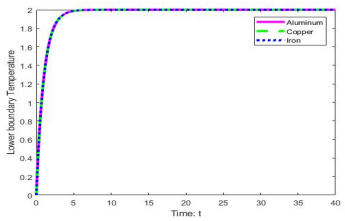

(a) Lower Boundary Temperature changes of heat sinks made of: aluminum, copper, and iron

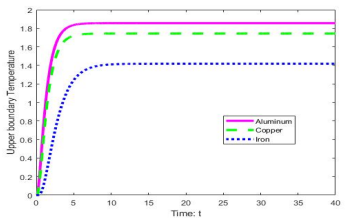

(b) Upper Boundary Temperature changes of heat sinks made of: aluminum, copper, and iron

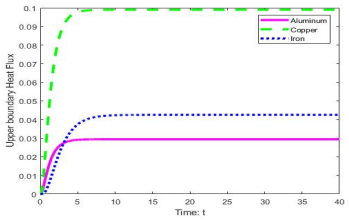

(c) The heat flux close to the upper boundary of heat sinks: aluminum, copper, and iron

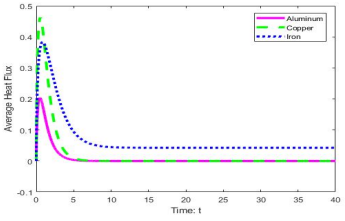

(d) Average heat flux of the heat sink interior body(excluding boundaries): aluminum, copper, and iron

Figure 5.1: Comparison of the cooling effect of three metal materials: aluminum, copper and iron. All placed in the piped water cooling environment

This was calculated by taking the temperature difference between the value at the top boundary point and the point 0.01 lower than the boundary, divided by the length 0.01 and times the value of k for each metal. This calculation was used instead of multiply the heat transfer coefficient with the upper boundary temperature,because the heat convection process is not consistent with conduction process. And we are aimed at comparing the difference among all the three interior space. Therefore we exclude the influence of the boundaries to keep the continuity property. So here we calculate the heat flux close to the top boundary but not on the top boundary.

In this graph 5.1c, the curve that reaches highest value represents copper. This is not surprising, because based on data from Table 6 we know that copper is really fast in conducting heat, comparing to the other two types of metal.

The average heat flux was calculated by take the difference of heat flux closed to the upper endpoint from the heat flux close to the lower endpoint. As stated in the previous paragraph, to keep the consistency of the system, we exclude the boundary points when calculate flux close to boundaries. In graph 5.1d, all three cures raise rapidly due to the pure conduction process along the bar then reduced because the absorbed energy reached the upper boundary and convection cooling started to work after around 3 seconds. We can see that aluminum is the first one to drop back to zero, copper is the second to drop back to zero, whereas iron is the third one to drop but did not reach zero at the end. These demonstrate that both copper and aluminum are good heat conductors and copper can transmit more energy away within the same time interval. The zero flux means the steady state of the interior system when heat flux in equals flux out. The positive average heat flux difference of iron means that the heat sink itself is absorbing heat and cannot reduce the energy as efficiently as copper bar and aluminum bar. We can conclude that

copper has the highest heat conduction efficiency, aluminum the second, whereas iron is not efficient enough to cool the heat source.

We have found out that copper is a better heat conductor than aluminum. However copper is heavier and more expensive than aluminum. By calculating the ratio between the two density: $8940/2712 = 3.2965$, we see that for every unit volume, copper is 3.2 times heavier thank aluminum. This is apparently not appealing for small electronic devices.

5.3 Further Discussions

There are many directions to expand the model. Due to the length limit and purpose of this report, here only list a few brief description about possible further explorations.

The Accuracy of Governing laws Modern technologies have assisted more accurate observations. In high heat flux and high unsteady system, the Fourier law is no longer accurate. One proposed relation is the *CV Constitutive Relation*:

$$\mathbf{q}(\mathbf{r},t) + \tau_0 \frac{\partial \mathbf{q}(\mathbf{r},t)}{\partial t} = -k \nabla T(\mathbf{r},t),$$

where τ_0 is a positive number related to the material, called *relaxation time*. This new relation can turn the original heat equation to hyperbolic and can be further generalized to approximate situations with longer time intervals and higher accuracy. More details can be found in the book by Wang [13, p19-25].

Higher Dimension We only examined the heat sink in one-dimension in space. The observed results from our Dirichlet-Robin simulation suggests that a model in two-dimension space could give a better modeling of the system cooled by air flow. And many other topics concerning the optimization of shape and heat efficiency could be explored.

6 Conclusion

This report has investigated the process and reasoning of building mathematical physical model from a simplified thermal conduction phenomenon. We have used one of the most commonly produced and studied object heat sinks. By proving and applying several important physical governing rules, we are able to understand that the process of maths modeling is to build up a globally true relations in space and time from a local situation-the studied heat transmitting in heat sinks. From the local properties of events, we use differential equations to formulate a relationship that holds globally in space and time. Those are the modeling equations (1a), (1b), (1c) and (1d) obtain in the problem formulation section. Certain boundaries and initial conditions are functioning as filters to find the appropriate solution that can approach the special local event from a group of general and global ones. We applied non-dimensionalisation to original model to remove the measure units so the equations hold under different space and time scheme.

Once we have the model, numerical approach is preferred because of the complexity of analytical approaches. Additionally analytical solutions exist only for some well-posed

questions and such low existance situation cannot assist to give inspirations of many real life models. We choose the Crank-Nicolson finite difference due to its reliable accuracy. A matrix system was then derived with the implicit method and codes were written in MatLab for simulation.

The simulations show that the best modeling is using Dirichlet on lower boundary and Robin on upper boundary. This combination gives a rather reliable resemblance of the heat sink in real life. Additionally we simulated and studied the different cooling effect when our modelled heat sink placed in four forced fluids flowing cooling systems: slow air flow, fast air flow, fast water flow in pipes and fast liquid flow in pipes. Water is a good choice for our 1-D model but simulation suggests that fast air flow can be a reasonably good cooling environment when we examine it in a 2-D model.

Furthermore, we added extra simulations in comparing the cooling effect when the sink (placed in the same cooling fluid) is made of different types of metal: aluminum, copper and iron. Results show that copper is better than aluminum but is much heavy and expensive than the latter. Additionally, iron is not efficient enough to reduce the temperature of the whole system. Even though aluminum is less efficient, it still guarantees that the system will not get over the safe temperature, since the total heat flux can maintain at a steady state.

References

[1] Adkins, C.J., 1987.*An introduction to thermal physics*. Cambridge : Cambridge University Press.

[2] Bejan, Adrian. 2013. *Convection Heat Transfer (4th Edition)* - 1. Fundamental Principles. John Wiley Sons. Online version available at:(https://app.knovel.com/hotlink/pdf/id:kt011B6VED/convection-heat-transfer/fundamental-principles)

[3] Computer Hope, 2017, *Heat Sink*[online]. Salt Lake City, Utah [cited 20 Feburary 2018]. Available from world wide web: (https://www.computerhope.com/jargon/h/heatsink.htm).

[4] Chu, R.C., Simons, R.E., Ellsworth, M.J., Schmidt, R.R. and Cozzolino, V., 2004. *Review of cooling technologies for computer products. Device and Materials Reliability*, IEEE Transactions on, 4(4), pp. 568-585.

[5] Emmons, C., 2016. *Newton's Law of Cooling*. Journal of Humanistic Mathematics, 6(1), p. 298.

[6] Flueck, Alexander J. 2005. *ECE 100*[online]. Chicago: Illinois Institute of Technology, Electrical and Computer Engineering Department, 2005 [cited 30 August 2005]. Available from World Wide Web: (http://www.ece.iit.edu/ flueck/ece100).

[7] Jiji, L.M., 2009. *Heat conduction. 3rd ed* Heidelberg: Berlin, Springer-Verlag.

[8] Jost, J., 2002. *Partial Differential Equations*. New York, NY: Springer New York.

[9] Simmons G.F., 1996 *Calculus with Analytic Geometry 2nd Edition*. Colorado: The McGraw-Hill Companies.

[10] Smith, G. 1985 *Numerical Solution of Partial Differential Equations: Finite Difference Methods, third edition*. Clarendon Press, Oxford.

[11] Taler, J. and Duda, P., 2006. *Solving Direct and Inverse Heat Conduction Problems*. Berlin, Heidelberg: Springer Berlin.

[12] Thomas, J.W., 1995. *Numerical Partial Differential Equations: Finite Difference Methods*. New York, NY : Springer New York.

[13] Wang, L., 2008. *Heat conduction : mathematical models and analytical solutions*. Berlin: Springer.

[14] Zhang, G., Liu, Z. and Wang, C., 2013. *A One- Dimensional Heat Transfer Model Analysis of Heat Sinks*. Heat Transfer Engineering, 35(6-8).

[15] Engineers Edge LLC. *Convective Heat Transfer Coefficients Table Chart*[online]. [cited 11 March 2018]. Available from World Wide Web: (https://www.engineersedge.com/heat_transfer/convective_heat_transfer_coefficients_13378.htm)

[16] Engineering ToolBox, (2005). *Thermal Conductivity of Metals*[online]. [Accessed 11 March 2018]. Available at: (https://www.engineeringtoolbox.com/thermal-conductivity-metals-d_858.html)

[17] Engineering ToolBox, (2004). *Metals and Alloys - Densities*[online]. [Accessed 11 March 2018] Available at: (https://www.engineeringtoolbox.com/metal-alloys-densities-d_50.html)

[18] Engineering ToolBox, (2003). *Specific Heats for Metals*[online]. [Accessed 11 March 2018]Available at: (https://www.engineeringtoolbox.com/specific-heat-metals-d_152.html)

7 Appendix A: Derivation of the Ruling Laws in Physics

Mathematical models are derived based on those fundamental physical laws mentioned in page 5. "Based on fundamental physical laws, the next approach is to develop relations among different physical variables for an arbitrary material system and process. Note that physical quantities for the system and the process are normally integrals. Using this approach, the physical lasws first lead to equations in a form in which some integrals are qual to zero. Bothe the continuity of the integrands and the localization theorem are then used to conclude that the integrands must be zero. This leads to the desired differential equation governing the local and instant relaitions among variables." [13] Therefore, below gives the detail proofs of deriving those maths equations from each given physical laws.

7.1 Proof of the Fourier's Law of heat conduction

In the following graph, Figure 7.1 the left hand side of the wall surface has temperature is T_{si} and that of the right hand side wall surface is T_{so}. To total width of the wall is L and both the left and right surface have equal area A. We assume that $T_{si} > T_{so}$.

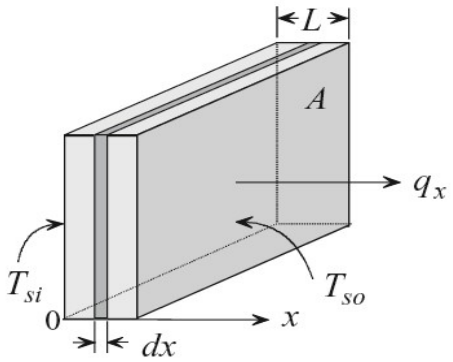

Figure 7.1: Fourier's law of conduction.[7, p3]

Therefore the reduce of energy at x_{si} equal to the increase of energy at x_{s0}. We have the following relation:

$$Q_x \propto A(T_{si} - Tso)/L \tag{7.1}$$

From the definition and equation 7.4 of heat capacity, we have the relation:

$$Q_x = c_v A(T_{si} - T_{so})/L. \tag{7.2}$$

Let the temperature be a dependent on x - $T(x)$ and define the vector $\mathbf{q}$ be the hear flow rate per unit surface area pointing from higher temperature to lower temperature. We change the right hand side according to a flow direction notation, we have the new equation:

$$q_x A = -c_v \frac{A(T(x_{s0}) - T(x_{si}))}{L} \tag{7.3}$$

Now change the length of L to a small quantity Δx, and cancel out the two A on both side of the equation:

$$q_x = -c_v \frac{A(T(x_0 + \Delta x) - T_{x_0})}{\Delta x} \tag{7.4}$$

Take the limit, we have the x-axis component of vector $\mathbf{q}$: $q_x = -c_v \partial_x T$. Using k to replace c_v, we have the Fourier's Law:

$$\mathbf{q} = -k \nabla T \tag{7.5}$$

This equation means that the flow of heat is opposite to the direction of temperature gradient.

7.2 Some Relevant Maths Theorems

Theorem 7.2.1 (Divergence Theorem) *(Also called Gauss's Theorem) states that the flux of a vector field $\boldsymbol{F}$ out through a closed surface S equals the integral of the divergence of $\boldsymbol{F}$ over the region R bounded by S:*

$$\iint_S \boldsymbol{F} \cdot \boldsymbol{n} \, dA = \iiint_R \nabla \boldsymbol{F} \, dV, \tag{7.6}$$

where $\nabla = \boldsymbol{i}\frac{\partial}{\partial x} + \boldsymbol{j}\frac{\partial}{\partial y} + \boldsymbol{k}\frac{\partial}{\partial z}$.

The vectors in **F** are perpendicular to the surface S. There this means the outward flux of **F** over the entire area A can be approximated by the sum of the divergence of **F** over the entire volume. [9, p775]

7.3 Proof of the equation for Conservation of Energy

If we want to the increase of temperature of a system by T, the energy need Q is apparently proportional to the mass M of the system: $Q \propto MT$. Referring to the definition of heat capacity and its relation equation (7.4) with Energy and temperature change: $Q = CMT$, where the mass variable M can be expressed by the product of density and volume: $M = \rho V$. Therefore we have the relation between volume and energy change:

$$Q = \rho CT\Delta V. \tag{7.7}$$

The total energy of the sytem thus can be expressed by integration:

$$E = \int_V \rho CT\, dV + \int_V f\, dV, \tag{7.8}$$

where f is the energy producing function within the system. If we do not have any inner energy production, we have $f = 0$.

Since we know the energy of a system can either stay constant within the system, or receive energy from another system or lose energy by transmitting its own to another system with the change of time t. The conservation of energy can be expressed by:

$$\frac{d}{dt}U = -\int_S \mathbf{qn}\, dS, \tag{7.9}$$

meaning the change of inner energy equals to the total change caused by heat flux through the entire surface. Substituting the equation (7.8) to the integral (7.3) gives:

$$\frac{d}{dt}\int_V \rho CT\, dV = \underbrace{-\int_S \mathbf{qn}\, dS}_{termA}, \tag{7.10}$$

With respect to the Divergence Theorem 7.2.1, the term A in equation (7.3) is equal to:

$$term\ A = -\int_V \nabla\mathbf{q}\, dV \tag{7.11}$$

Therefore, equation (7.3) becomes:

$$\int_V \rho C\partial_t T\, dV = -\int_V \nabla\mathbf{q}\, dV \tag{7.12}$$

This indicates the equatin:

$$\partial_t T + \nabla\mathbf{q} = 0 \tag{7.13}$$

This equation (7.13) represents the conservation of energy for a homogeneous system i.e when there is no external heat flux entering the system. When there is external heat entering from some location, we have the following equation:

$$\partial_t T + \nabla\mathbf{q} = f \tag{7.14}$$

7.4 Some relevant physical definitions

Heat capacity C is the measure of the amount of heat (symble Q) or energy needed to increase a system's temperature by a certain unit ΔT:

$$Q = C \cdot \Delta T \tag{7.15}$$

To be more precise, this is measuring the temperature change in a simple system which has two degrees of freedom. We can only have one dependent variable over one domain. therefore the system expressed by equation (7.4) needs one fixed constraint by putting suffix under the variable C:

$$C_p = Q/\Delta T, \tag{7.16}$$

This is the heat capacity with a constant pressure. And similarly the capacity with a fixed volume:

$$C_v = Q/\Delta T, \tag{7.17}$$

[1, p23]

Solidus Notation A physical quantity contains a value and a unit. For example, the mass m_e of the electron is given by:

$$m_e = 9.11 \times 10^{-31}\ \ kg \tag{7.18}$$

Definition 7.4.1 *An equivalent notation of the above equation is:*

$$m_c/kg = 9.11 \times 10^{-31} \tag{7.19}$$

This is the solidus notation. It now using the division of a physical quantity by it's unit giving a pure number. Complex equations involving physical quantities should often be written in this concise and unambiguous solidus notation to keep involved quantities dimensionless. This is due to the reason that equations are representing a true physical fact that is true regardless of how a quantities being measured or in which unit is being measured. Therefore those quantities need to be dimensionless in mathematical equations.

[1, p viii]

8 Appendix B: Detailed process of the Non-Dimensionalisation of our Model

Here shows the calculation details for the non-dimesionalisation equations (2.2) in page 9. Here are the original model:

$$\partial_t T = K\partial_{zz} T, \tag{1a}$$
$$T(z,0) = T_\infty, \tag{1b}$$
$$T(0,t) = T_\infty + D(1 - e^{-t/\tau}), \tag{1c}$$
$$\frac{hT}{k} + \partial_z T(L,t) = \frac{h}{k} T_\infty, \tag{1d}$$

First step is to take the influence of room temperature away from our function of T. By defining $T^{'} = T - T_\infty$, substituting $T = T^{'} + T_\infty$ back to the original models (1a), (1b), (1c), and (1d), we have the following equations:

$$\partial_t(T^{'} + T_\infty) = K\partial_{zz}(T^{'} + T_\infty), \tag{8.1}$$
$$T^{'}(z,0) + T_\infty = T_\infty, \tag{8.2}$$
$$T^{'}(0,t) + T_\infty = T_\infty + D(1 - e^{-t/\tau}), \tag{8.3}$$
$$\frac{h(T^{'} + T_\infty)}{k} + \partial_z(T^{'}(L,t) + T_\infty) = \frac{h}{k}T_\infty \tag{8.4}$$

With some basic algebra manipulations, we have:

$$\partial_t T^{'} = K\partial_{zz}T^{'}, \tag{8.5}$$
$$T^{'}(z,0) = 0, \tag{8.6}$$
$$T^{'}(0,t) = D(1 - e^{-t/\tau}), \tag{8.7}$$
$$\frac{hT^{'}}{k} + \partial_z T^{'}(L,t)) = 0. \tag{8.8}$$

Second step is to find typical units for temperature. We notice that from equation (8.7), the range of $T^{'}$ is from 0 to D, *i.e.* $[T^{'}] = D$. From the domain of $z \in [0, L]$, we have $[z] = L$, from the interval of time $t \in [0, \tau]$. Therefore we need to remove all the influence of D, L, and τ by introducing the varialbes: $T^* = T^{'}/D$, $z^* = z/L$, $t^* = t/\tau$.

$$\partial_t T^{'} = \lim_{\Delta t \to 0} \frac{T^{'}(t + \Delta t) - T^{'}(t)}{\Delta t} = D \lim_{\Delta t \to 0} \frac{T^*(t + \Delta t) - T^*(t)}{\Delta t} \tag{8.9}$$
$$= D\partial_t T^* = D\frac{\partial T^*}{\partial t^*}\frac{dt^*}{dt} = \frac{D}{\tau}\partial_{t^*}T^*, \tag{8.10}$$

where $\frac{dt^*}{dt} = \frac{1}{\tau}$. Now use the relation between z and z^*, using chain rule we have:

$$\frac{\partial T^{'}}{\partial z^*} = \partial_{z^*}T\frac{dz}{dz^*} = \frac{\partial_{z^*}T^{'}}{L}. \tag{8.11}$$

Using the calculation in equations (8.10) and (8.11), we have the following equation for changing $\partial_{zz}T'$to $\partial_{z^*z^*}T^*$:

$$\partial_{zz}T^{'} = D\partial_{zz}T^* = D\partial_{z^*z^*}T^*/L^2 \tag{8.12}$$

Subtract those equations (8.10), (8.11) and (8) to our model system (equations (8.5),(8.6), (8.7) and (8.8)) and remove all the $*$ signs gives:

$$\partial_t T = F_0\partial_{zz}T, \tag{2a}$$
$$T(z,0) = 0, \tag{2b}$$
$$T(0,t) = 1 - e^{-t}), \tag{2c}$$
$$B_i T(1,t) + \partial_z T(1,t)) = 0, \tag{2d}$$

where $F_0 = \frac{k\tau}{\rho c L^2}$, and $B_i = \frac{hL}{k}$.

9 Appendix I: MatLab Scripts

This section involves MatLab scripts for the numeriacal approaches.

9.1 Code forValidity Checking

```
% Validation simulation
close all
clear
clc
dz = .01;
dt = .01;
ck =  0.204 ; %thermal conductivity  KJ/(s mK), 1W = 0.001 KJ/s
cd =  2712*1000; % density g/(m^3)
cc = 0.91/1000;% specific heat KJ/gK
cl = 0.01;% m
Fo = ck/(cd*cc*cl*cl); %Fourier Number
mode = 3;
%%
alpha = dt*Fo/(2*dz^2);
zVec = 0:dz:1;
tVec = 0:dt:10;
nz = length(zVec)-1;
nt = length(tVec)-1;
PhiMat = zeros(nz+1,nt+1);%Matrix where we record the results
PhiMat(:,1) = cos(mode*pi*zVec);
% Neumann-Neumann
B = diag(-2*ones(1,nz+1))+diag(ones(1,nz),-1)+diag(ones(1,nz),1);
B(1,2) = 2;
B(end,end-1) = 2;
B1 = (eye(nz+1)-alpha*B)^(-1);
B2 = B1*(eye(nz+1)+alpha*B);
B1 = 2*dz*alpha*B1;
gb = zeros(size(tVec));
gt = zeros(size(tVec));
for kk = 1:nt
    kk/nt
    PhiMat(:,kk+1) = B2*PhiMat(:,kk)+B1*...
        [gb(kk)+gb(kk+1);zeros(nz-1,1);gt(kk)+gt(kk+1)];
end
figure
surf(tVec,zVec,PhiMat,'LineStyle','none','FaceColor','interp')
set(gca,'FontSize',16)
ylabel('$z/L$','interpreter','Latex','FontSize',24)
xlabel('$t/\tau$','interpreter','Latex','FontSize',24)
figure
plot(zVec,cos(mode*pi*zVec).*exp(-mode^2*pi^2*Fo*tVec(end)),'+')
hold on
plot(zVec,PhiMat(:,end),'x')
error = cos(mode*pi*zVec').*exp(-mode^2*pi^2*Fo*tVec(end))-PhiMat(:,end);
plot(zVec,error)
errorL2 = mean(error(1:end-1).^2)
```

9.2 Simulation code for Dirichlet-Dirichlet

```
%Dirichlet condition
close all
clear
clc
dz = .01;
dt = .01;
ck =  0.204 ; %thermal conductivity  KJ/(s mK), 1W = 0.001 KJ/s
cd =  2712; % density kg/(m^3)
cc = 0.91;% specific heat KJ/kgK
cl = 0.01;% m
Fo = ck/(cd*cc*cl*cl); %Fourier Number
%%
alpha = dt*Fo/(2*dz^2);
zVec = 0:dz:1;
tVec = 0:dt:40;
nz = length(zVec)-1;
nt = length(tVec)-1;
PhiMat = zeros(nz+1,nt+1);%Matrix where we record the results
```

```
%Dirichlet-Dirichlet
A = diag(-2*ones(1,nz-1))+diag(ones(1,nz-2),-1)+diag(ones(1,nz-2),1);
A1 = (eye(nz-1)-alpha*A)^(-1);
A2 = eye(nz-1)+alpha*A;
PhiMat(1,2:end) = 2*(1-exp(-tVec(2:end)));
PhiMat(end,2:end) = (1-exp(-tVec(2:end)));
for kk = 1:nt
    kk/nt
    PhiMat(2:end-1,kk+1) = A1*A2*PhiMat(2:end-1,kk)+alpha*A1*...
        [PhiMat(1,kk)+PhiMat(1,kk+1);zeros(nz-3,1);...
        PhiMat(end,kk)+PhiMat(end,kk+1)];
end
figure
surf(tVec,zVec,PhiMat,'LineStyle','none','FaceColor','interp')
set(gca,'FontSize',16)
ylabel('$z/L$','interpreter','Latex','FontSize',24)
xlabel('$t/\tau$','interpreter','Latex','FontSize',24)
figure
contour(tVec,zVec,PhiMat)
```

9.3 Simulation code for Neumann-Neumann

```
% Neumann conditions
close all
clear
clc
dz = .01;
dt = .01;
Fo = 0.8266; %Fourier Number
%%
alpha = dt*Fo/(2*dz^2);
zVec = 0:dz:1;
tVec = 0:dt:40;
nz = length(zVec)-1;
nt = length(tVec)-1;
PhiMat = zeros(nz+1,nt+1);%Matrix where we record the results
% Neumann-Neumann
B = diag(-2*ones(1,nz+1))+diag(ones(1,nz),-1)+diag(ones(1,nz),1);
B(1,2) = 2;
B(end,end-1) = 2;
B1 = (eye(nz+1)-alpha*B)^(-1);
B2 = B1*(eye(nz+1)+alpha*B);
B1 = 2*dz*alpha*B1;
gb = 2*(1-exp(-tVec(1:end)));
gt = -2*(1-exp(-tVec(1:end)));
for kk = 1:nt
    kk/nt
    PhiMat(:,kk+1) = B2*PhiMat(:,kk)+B1*...
        [gb(kk)+gb(kk+1);zeros(nz-1,1);gt(kk)+gt(kk+1)];
end
figure
surf(tVec,zVec,PhiMat,'LineStyle','none','FaceColor','interp')
set(gca,'FontSize',16)
ylabel('$z/L$','interpreter','Latex','FontSize',24)
xlabel('$t/\tau$','interpreter','Latex','FontSize',24)
```

9.4 Simulation code for Dirichlet-Robin

```
%Dirichlet and Robin
close all
clear
clc
dz = .01,dt = .01,ck =  0.204;%thermal conductivity  KJ/(s mK), 1W = 0.001 KJ/s
cd =  2712; % density kg/(m^3)
cc = 0.91;% specific heat KJ/kgK
cl = 0.01;% m
Fo = ck/(cd*cc*cl*cl); %Fourier Number
ch = 10; % take value of 0.01; 0.1; 3 ; 10
Bi = ch * cl/ck;  %Biot Number
alpha = dt*Fo/(2*dz^2);
zVec = 0:dz:1;
tVec = 0:dt:40;
nz = length(zVec)-1;
nt = length(tVec)-1;
PhiMat = zeros(nz+1,nt+1);%Matrix where we record the results
```

```
%Dirichlet-Robin
C = diag(-2*ones(1,nz))+diag(ones(1,nz-1),-1)+diag(ones(1,nz-1),1);
C(end,end-1) = 2;
C(end,end) = -2*(1+dz*Bi);
C1 = (eye(nz)-alpha*C)^(-1);
C2 = C1*(eye(nz)+alpha*C);
C1 = alpha*C1;
PhiMat(1,2:end) = 2*(1-exp(-tVec(2:end)));
for kk = 1:nt
    kk/nt
    PhiMat(2:end,kk+1) = C2*PhiMat(2:end,kk)+C1*...
        [PhiMat(1,kk)+PhiMat(1,kk+1);zeros(nz-1,1)];
    PhiMat(end,kk+1) = PhiMat(end-2,kk+1)/(1+2*dz*Bi);
end
figure
surf(tVec,zVec,PhiMat,'LineStyle','none','FaceColor','interp')
set(gca,'FontSize',16)
ylabel('$z/L$','interpreter','Latex','FontSize',24)
xlabel('$t/\tau$','interpreter','Latex','FontSize',24)
```

9.4.1 Codes for ploting the boundary temperature change in different cooling fluid

```
% plotting all the four fluids effect together % plotting all the four fluids effect together
close all
clear
clc
load('PhiMatBi0.0004902.mat')
PhiMat1= PhiMat;
load('PhiMatBi0.004902.mat')
PhiMat2= PhiMat;
load('PhiMatBi0.14706.mat')
PhiMat3= PhiMat;
load('PhiMatBi0.4902.mat')
PhiMat4= PhiMat;
T1 = PhiMat1(end,:);
T2 = PhiMat2(end,:);
T3 = PhiMat3(end,:);
T4 = PhiMat4(end,:);
Tmax = PhiMat1(1,end);
tVec = 0:0.01:30;
figure
graph1 = plot(tVec,T1,'y',tVec,T2,'m--',tVec,T3,'c:',tVec, T4,'b-.');
hline = refline([0 Tmax]);
set(graph1,'LineWidth',3);
set(hline,'LineWidth',1.5)
hline.Color = 'r';
xlabel('Time: t')
ylabel('Change of Boundary Temperature along time')
legend('slow air flow','fast air flow','water','other liquid','Maximum Temperature')
```

9.4.2 Codes for ploting the boundary temperature change in bars of different length in air-flow cooling environment

```
close all
clear
clc
load('PhiMatLength0.01.mat')
PhiMat1= PhiMat;
load('PhiMatLength0.02.mat')
PhiMat2= PhiMat;
load('PhiMatLength0.03.mat')
PhiMat3= PhiMat;
load('PhiMatLength0.04.mat')
PhiMat4= PhiMat;
T1 = PhiMat1(end,:);
T2 = PhiMat2(end,:);
T3 = PhiMat3(end,:);
T4 = PhiMat4(end,:);
Tmax = PhiMat1(1,end);
tVec = 0:0.01:80;
figure
graph1 = plot(tVec,T1,'y',tVec,T2,'m--',tVec,T3,'c:',tVec, T4,'b-.');
hline = refline([0 Tmax]);
set(graph1,'LineWidth',3);
set(hline,'LineWidth',1.5)
hline.Color = 'r';
```

```
xlabel('Time: t')
ylabel('Upper Boundary Temperature')
legend('Length: 1cm','Length: 2cm','Length: 3cm','Length 4 cm','Maximum Temperature')
```

9.4.3 Plotting codes for three different heat sinks of different metal materials

```
close all
clear
clc
load('PhiMatBiMet0.07772.mat')
PhiMat1= PhiMat;
load('PhiMatBiMet0.14706.mat')
PhiMat2= PhiMat;
load('PhiMatBiMet0.41096.mat')
PhiMat3= PhiMat;
T1 = PhiMat1(end,:);
ck1 =  0.204;
T2 = PhiMat2(end,:);
ck2 = 0.386;
T3 = PhiMat3(end,:);
ck3 =0.073;
% UHF1=3*T1; % UHF2=3*T2; %UHF3=3*T3;
UHF1=ck1*(PhiMat1(end-1,:)-PhiMat1(end,:))/0.01;
UHF2=ck2*(PhiMat2(end-1,:)-PhiMat2(end,:))/0.01;
UHF3=ck3*(PhiMat3(end-1,:)-PhiMat3(end,:))/0.01;
LHF1 = ck1*(PhiMat1(1,:)-PhiMat1(2,:))/0.01;
LHF2 = ck2*(PhiMat2(1,:)-PhiMat2(2,:))/0.01;
LHF3 = ck3*(PhiMat3(1,:)-PhiMat3(3,:))/0.01;
tVec = 0:0.01:40;
%q1 upper surface heat flux
Q1UHF1 = ck1*(PhiMat1(25,:)-PhiMat1(26,:))/0.01;
Q1UHF2 = ck2*(PhiMat2(25,:)-PhiMat2(26,:))/0.01;
Q1UHF3 = ck3*(PhiMat3(25,:)-PhiMat3(26,:))/0.01;
%q2 upper surface heat flux
Q2UHF1 = ck1*(PhiMat1(50,:)-PhiMat1(51,:))/0.01;
Q2UHF2 = ck2*(PhiMat2(50,:)-PhiMat2(51,:))/0.01;
Q2UHF3 = ck3*(PhiMat3(50,:)-PhiMat3(51,:))/0.01;
%q3 upper surface heat flux
Q3UHF1 = ck1*(PhiMat1(75,:)-PhiMat1(76,:))/0.01;
Q3UHF2 = ck2*(PhiMat2(75,:)-PhiMat2(76,:))/0.01;
Q3UHF3 = ck3*(PhiMat3(75,:)-PhiMat3(76,:))/0.01;
nt = length(tVec);
figure
graph1 = plot(tVec,UHF1,'m',tVec,UHF2,'g--',tVec,UHF3,'b:');
set(graph1,'LineWidth',3);
xlabel('Time: t')
ylabel('Upper boundary Heat Flux')
legend('Aluminum','Copper','Iron')
figure
graph1 = plot(tVec,PhiMat1(1,:),'m',tVec,PhiMat2(1,:),'g--',tVec,PhiMat3(1,:),'b:');
set(graph1,'LineWidth',3);
xlabel('Time: t')
ylabel('Lower boundary Temperature')
legend('Aluminum','Copper','Iron')
figure
graph1 = plot(tVec,T1,'m',tVec,T2,'g--',tVec,T3,'b:');
set(graph1,'LineWidth',3);
xlabel('Time: t')
ylabel('Upper boundary Temperature')
legend('Aluminum','Copper','Iron')
figure
graph1 = plot(tVec,-UHF1+LHF1,'m',tVec,-UHF2+LHF2,'g--',tVec,-UHF3+LHF3,'b:');
set(graph1,'LineWidth',3);
xlabel('Time: t')
ylabel('Average Heat Flux')
legend('Aluminum','Copper','Iron')
figure
graph1 = plot(tVec,-UHF1+Q3UHF1,'m',tVec,-UHF2+Q3UHF2,'g--',tVec,-UHF3+Q3UHF3,'b:');
set(graph1,'LineWidth',3);
xlabel('Time: t')
ylabel('Average heat flux:q4')
legend('Aluminum','Copper','Iron')
figure
dz1 = 0.01*100/4;
graph1 = plot(tVec,-Q1UHF1+LHF1,'m',tVec,-Q1UHF2+LHF2,'g--',tVec,-Q1UHF3+LHF3,'b:');
set(graph1,'LineWidth',3);
```

```
xlabel('Time: t')
ylabel('Average heat flux: q1')
legend('Aluminum','Copper','Iron')
figure
graph1 = plot(tVec,-Q2UHF1+Q1UHF1,'m',tVec,-Q2UHF2+Q1UHF2,'g--',tVec,-Q2UHF3+Q1UHF3,'b:');
set(graph1,'LineWidth',3);
xlabel('Time: t')
ylabel('Average heat flux: q2')
legend('Aluminum','Copper','Iron')
figure
graph1 = plot(tVec,-Q3UHF1+Q2UHF1,'m',tVec,-Q3UHF2+Q2UHF2,'g--',tVec,-Q3UHF3+Q2UHF3,'b:');
set(graph1,'LineWidth',3);
xlabel('Time: t')
ylabel('Average heat flux: q3')
legend('Aluminum','Copper','Iron')
```

10 Appendix III: Nomenclature

Table 8: Nomenclature: notations and meanings used in the report

symbol	meaning
$\mathbf{n}$	outward normal vector on the surface
c	specific heat of the material
ρ	density of the material
U	inner energy
F	rate of internal energy generation per unit volume
k	thermal conductivity, measured in unit: $W/m \cdot K$
L	length of the heat sink metal measured in cm
$\mathbf{q}$	heat flux
T	Temperature
V	volumn of a body
A	Surface area of a body
Ω	internal system of a body
$\partial\Omega$	boundary surface of a body
K	notation of $\frac{k}{\rho c}$
α	notation of $\frac{1}{\rho c}$
$\varphi(M)$	initial temperature state of a system
h	the heat transfer coefficient
F_0	Fourier number: $(k\tau)/(\rho c L^2)$
B_i	Biot number $\frac{hL}{k}$: ratio of the heat transfer resistances inside vs resistance outside
τ	time scaling in seconds (s)